

Stress Concentration Around a Small Circular Hole in the HiMAT Composite Plate

William L. Ko

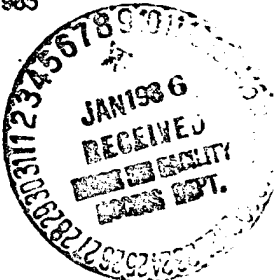
(NASA-TH-86038) STRESS CONCENTRATION AROUND
A SMALL CIRCULAR HOLE IN THE HiMAT COMPOSITE
PLATE (NASA) 18 F HC A02/ME A01 CSCL 11D

N86-1535J

Unclas
63/24 05090

DISTRIBUTION STATEMENT A
Approved for public release
Distribution Unlimited

December 1985



DEPARTMENT OF DEFENSE
ELASTICS TECHNICAL EVALUATION CENTER
BRADCOM, DOVER, N. J. 07801

NASA
National Aeronautics and
Space Administration

DTIC QUALITY INSPECTED 5

19951128 122

PLASTEC 49528

Stress Concentration Around a Small Circular Hole in the HiMAT Composite Plate

William L. Ko
Ames Research Center, Dryden Flight Research Facility, Edwards, California

1985

Accession For	
NTIS ORAM	<input checked="" type="checkbox"/>
DTIC TAB	<input type="checkbox"/>
Unannounced Justification	<input type="checkbox"/>
By _____ Distribution/	
Availability Codes	
Dist	Avail and/or Special
A-1	



National Aeronautics and
Space Administration
Ames Research Center
Dryden Flight Research Facility
Edwards, California 93523

SUMMARY

Anisotropic plate theory was used to calculate the anisotropic stress concentration factors for a composite plate (AS/3501-5 graphite/epoxy composite, single ply or laminated) containing a circular hole. This composite material was used on the highly maneuverable aircraft technology (HiMAT) vehicle. It was found that the anisotropic stress concentration factor could be greater or less than 3 (the stress concentration factor for isotropic materials), and that the locations of the maximum tangential stress points could shift with the change of fiber orientation with respect to the loading axis. The effect of hole size on the stress concentration factor was examined using the Point Stress Criterion and the Averaged Stress Criterion. The predicted stress concentration factors based on the two theories compared fairly well with the measured values for the hole size 0.3175 cm (1/8 in). It was also found that through the lamination process, the stress concentration factor could be reduced drastically, indicating an improvement in structural performance.

INTRODUCTION

When an infinite isotropic plate containing a circular hole is subjected to remote uniaxial tension, the tangential stress along the boundary of the circular hole will reach a value three times the remote tensile stress at two boundary points lying on the hole diameter perpendicular to the loading axis. Namely, the maximum tangential stress concentration factor is 3, which is independent of the hole size. For anisotropic materials, such as fiber-reinforced composite materials, the picture is entirely different. The value of the maximum tangential stress concentration factor for a composite plate can be greater or less than 3, and the locations of the maximum stress points could shift depending on the loading direction and the fiber orientations.

This report calculates the tangential stress distribution around a circular hole in a composite plate (single ply or laminated) and examines how the maximum stress points shift with the fiber orientations. In addition, the dependency of the stress concentration factor on the hole size is examined. In the analysis, the composite system is treated as a continuous anisotropic plate having effective elastic properties. The calculated stress concentration factors are then compared with experimental data.

NOMENCLATURE

- | | |
|-------|---|
| a_0 | small fixed distance ahead of the hole boundary used in the Average Stress Criterion |
| d_0 | characteristic distance ahead of the hole boundary used in the Point Stress Criterion |
| E_1 | modulus of elasticity of single ply in axis-1 direction or modulus of elasticity of anisotropic plate in axis-1 direction |

E_2	modulus of elasticity of single ply in axis-2 direction or modulus of elasticity of anisotropic plate in axis-2 direction
\bar{E}_1	modulus of elasticity of laminated composite plate in axis-1 direction
\bar{E}_2	modulus of elasticity of laminated composite plate in axis-2 direction
E_a	modulus of elasticity of anisotropic plate in a direction
E_L	modulus of elasticity of single ply in fiber direction
E_T	modulus of elasticity of single ply transverse to fiber direction
G_{12}	shear modulus of single ply associated with {1,2} system
G_{LT}	shear modulus of single ply associated with {L,T} system
K	stress concentration factor
$K_{\pi/2}$	stress concentration factor at $\alpha = \pi/2$
k	$= \sqrt{\frac{E_1}{E_2}}$
L	coordinate axis in fiber direction
N	number of composite layers
R	radius of circular hole
x, y	rectangular Cartesian coordinates
T	coordinate axis transverse to fiber direction
{1,2}	rectangular coordinate system
α	angular coordinate
θ	angle between axis 1 and axis L
μ_1, μ_2	complex roots of the anisotropic plate characteristic equation
ν_{12}, ν_{21}	Poisson's ratios of single ply with respect to {1,2} system
ν_{LT}	Poisson's ratio of single ply with respect to {L,T} system
$\bar{\nu}_{12}, \bar{\nu}_{21}$	Poisson's ratios of laminated composite plate with respect to {1,2} system
ξ_1	$R/(R + d_0)$

ξ_2	$R/(R + a_0)$
σ_α	stress in α direction
σ_f	tensile strength of composite plate
σ_∞	remote tensile stress
σ_y	stress in y direction

COMPOSITE ELASTIC CONSTANTS

Let axes {1,2} be the coordinate axes, and let axes {L,T} be the principal elastic or material axes of the single composite ply shown in figure 1. The ply-elastic constants $\{E_1, E_2, G_{12}, \nu_{12}, \nu_{21}\}$ with respect to the {1,2} system can be related to the material constants $\{E_L, E_T, G_{LT}, \nu_{LT}, \nu_{TL}\}$ with respect to the {L,T} system through the following equations (refs. 1 and 2).

$$E_1 = E_L \left/ \left[\cos^4 \theta + \frac{E_L}{E_T} \sin^4 \theta + \frac{1}{4} \left(\frac{E_L}{G_{LT}} - 2\nu_{LT} \right) \sin^2 2\theta \right] \right. \quad (1)$$

$$E_2 = E_L \left/ \left[\sin^4 \theta + \frac{E_L}{E_T} \cos^4 \theta + \frac{1}{4} \left(\frac{E_L}{G_{LT}} - 2\nu_{LT} \right) \sin^2 2\theta \right] \right. \quad (2)$$

$$G_{12} = E_L \left/ \left[1 + 2\nu_{LT} + \frac{E_L}{E_T} - \left(1 + 2\nu_{LT} + \frac{E_L}{E_T} - \frac{E_L}{G_{LT}} \right) \cos^2 2\theta \right] \right. \quad (3)$$

$$\nu_{12} = \frac{E_1}{E_L} \left[\nu_{LT} - \frac{1}{4} \left(1 + 2\nu_{LT} + \frac{E_L}{E_T} - \frac{E_L}{G_{LT}} \right) \sin^2 2\theta \right] \quad (4)$$

$$\nu_{21} = \frac{E_2}{E_L} \left[\nu_{LT} - \frac{1}{4} \left(1 + 2\nu_{LT} + \frac{E_L}{E_T} - \frac{E_L}{G_{LT}} \right) \sin^2 2\theta \right] \quad (5)$$

If the composite plate is made of N number of single plies with different fiber orientations, then by using the mixture rule, the engineering elastic constants $\{\bar{E}_1, \bar{E}_2, \bar{G}_{12}, \bar{\nu}_{12}, \bar{\nu}_{21}\}$ for the composite plate can be written as

$$\bar{E}_1 = \frac{1}{N} \sum_{j=1}^N E_1(\theta_j) \quad (6)$$

$$\bar{E}_2 = \frac{1}{N} \sum_{j=1}^N E_2(\theta_j) \quad (7)$$

$$\bar{G}_{12} = \frac{1}{N} \sum_{j=1}^N G_{12}(\theta_j) \quad (8)$$

$$\bar{\nu}_{12} = \frac{1}{N} \sum_{j=1}^N \nu_{12}(\theta_j) \quad (9)^*$$

$$\bar{\nu}_{21} = \frac{1}{N} \sum_{j=1}^N \nu_{21}(\theta_j) \quad (10)^*$$

The HiMAT composite plate (A5/3501-5 graphite/epoxy composite) is made up of 34 plies (N = 34, ply thickness = 0.0133 cm (0.00525 in)) with the following fiber orientations:

14 plies of $\theta = +50^\circ$ fiber orientation

14 plies of $\theta = -50^\circ$ fiber orientation

6 plies of $\theta = +35^\circ$ fiber orientation

The ply engineering elastic constants with respect to the principal elastic axes {L,T} are given by

$$E_L = 137.90 \text{ GPa} (20 \times 10^6 \text{ lb/in}^2) \quad (11)$$

$$E_T = 10.27 \text{ GPa} (1.49 \times 10^6 \text{ lb/in}^2) \quad (12)$$

$$G_{LT} = 2.41 \text{ GPa} (0.35 \times 10^6 \text{ lb/in}^2) \quad (13)$$

$$\nu_{LT} = 0.3 \quad (14)$$

Using equations (11) to (14), the ply elastic constants with respect to axes {1,2} can be calculated from equations (1) to (5). For $\theta = \pm 50^\circ$ fiber orientations,

$$E_1(\pm 50^\circ) = 7.45 \text{ GPa} (1.0809 \times 10^6 \text{ lb/in}^2) \quad (15)$$

$$E_2(\pm 50^\circ) = 8.43 \text{ GPa} (1.2237 \times 10^6 \text{ lb/in}^2) \quad (16)$$

$$G_{12}(\pm 50^\circ) = 8.46 \text{ GPa} (1.2274 \times 10^6 \text{ lb/in}^2) \quad (17)$$

$$\nu_{12}(\pm 50^\circ) = 0.5676 \quad (18)$$

For $\theta = +35^\circ$ fiber orientation,

$$E_1(+35^\circ) = 9.59 \text{ GPa} (1.3904 \times 10^6 \text{ lb/in}^2) \quad (19)$$

$$E_2(+35^\circ) = 7.40 \text{ GPa} (1.0732 \times 10^6 \text{ lb/in}^2) \quad (20)$$

$$G_{12}(+35^\circ) = 6.91 \text{ GPa} (1.0025 \times 10^6 \text{ lb/in}^2) \quad (21)$$

*Note that the mixture rule does not give the relationship $\bar{\nu}_{12}\bar{E}_2 = \bar{\nu}_{21}\bar{E}_1$.

$$\nu_{12}(+35^\circ) = 0.6671 \quad (22)$$

Using equations (15) to (18) and equations (19) to (22), the engineering elastic constants for the HIMPT composite plate with respect to {1,2} system, can be calculated from equations (6) to (9).

$$\begin{aligned} \bar{E}_1 &= \frac{14}{34} E_1 (+50^\circ) + \frac{14}{34} E_1 (-50^\circ) + \frac{6}{34} E_1 (+35^\circ) \\ &= 7.83 \text{ GPa } (1.1356 \times 10^6 \text{ lb/in}^2) \end{aligned} \quad (23)$$

$$\begin{aligned} \bar{E}_2 &= \frac{14}{34} E_2 (+50^\circ) + \frac{14}{34} E_2 (-50^\circ) + \frac{6}{34} E_2 (+35^\circ) \\ &= 8.25 \text{ GPa } (1.1972 \times 10^6 \text{ lb/in}^2) \end{aligned} \quad (24)$$

$$\begin{aligned} \bar{G}_{12} &= \frac{14}{34} G_{12} (+50^\circ) + \frac{14}{34} G_{12} (-50^\circ) + \frac{6}{34} G_{12} (+35^\circ) \\ &= 8.19 \text{ GPa } (1.1877 \times 10^6 \text{ lb/in}^2) \end{aligned} \quad (25)$$

$$\bar{\nu}_{12} = \frac{14}{34} \nu_{12} (+50^\circ) + \frac{14}{34} \nu_{12} (-50^\circ) + \frac{6}{34} \nu_{12} (+35^\circ) = 0.5851 \quad (26)$$

TANGENTIAL STRESS AROUND A CIRCULAR HOLE

For an anisotropic plate containing a circular hole subjected to remote uniaxial tensile stress σ_∞ , acting at an angle ϕ with respect to the principal elastic axis 1 of the plate (fig. 2), the tangential stress, σ_α (or tangential stress concentration factor, $K \equiv \sigma_\alpha/\sigma_\infty$) along the circular hole boundary may be expressed as (ref. 3, p. 174)

$$\begin{aligned} K \equiv \frac{\sigma_\alpha}{\sigma_\infty} &= \frac{E_\alpha}{E_1} \left\{ [-\cos^2 \phi + (k+n) \sin^2 \phi] k \cos^2 \alpha \right. \\ &\quad + [(1+n) \cos^2 \phi - k \sin^2 \phi] \sin^2 \alpha \\ &\quad \left. - n (1 + k + n) \sin \phi \cos \phi \sin \alpha \cos \alpha \right\} \end{aligned} \quad (27)$$

where E_α is the modulus of elasticity in the α direction (fig. 2) given by

$$\frac{E_\alpha}{E_1} = 1 / \left[\sin^4 \alpha + \frac{E_1}{E_2} \cos^4 \alpha + \frac{1}{4} \left(\frac{E_1}{G_{12}} - 2\nu_{12} \right) \sin^2 2\alpha \right] \quad (28)$$

where k and n are defined by

$$k \equiv -\mu_1 \mu_2 = \sqrt{\frac{E_1}{E_2}} \quad (29)$$

$$n \equiv -i(\mu_1 + \mu_2) = \sqrt{2\left(\frac{E_1}{E_2} - \nu_{12}\right) + \frac{E_1}{G_{12}}} \quad (30)$$

where $i \equiv \sqrt{-1}$, and μ_1 and μ_2 are the complex roots of the anisotropic plate characteristic equation

$$\mu^4 + \left(\frac{E_1}{G_{12}} - 2\nu_{12}\right) \mu^2 + \frac{E_1}{E_2} = 0 \quad (31)$$

For isotropic materials $k = 1$ and $n = 2$, and the stress concentration factor K (eq. (27)) reduces to

$$K = \frac{\sigma_\alpha}{\sigma_\infty} = 1 - 2 \cos 2(\alpha - \phi) \quad (32)$$

which gives $K = -1$ at $(\alpha - \phi) = 0$ or π , and $K = 3$ at $(\alpha - \phi) = \pm \pi/2$

HOLE SIZE EFFECT

Consider a circular hole of radius R in an infinite anisotropic plate as shown in figure 3. If the remote uniform stress σ_∞ is applied in the y -axis (or axis 1) direction, then the normal stress σ_y in the y -axis direction at a point on the x -axis (or axis 2) in front of the hole may be approximated by (ref. 4)

$$\begin{aligned} \sigma_y(x,0) = \frac{\sigma_\infty}{2} \left\{ 2 + \left(\frac{R}{x}\right)^2 + 3\left(\frac{R}{x}\right)^4 \right. \\ \left. - [(1+n) - 3] \left[5\left(\frac{R}{x}\right)^6 - 7\left(\frac{R}{x}\right)^8 \right] \right\} \quad (33) \\ (x > R) \end{aligned}$$

At the hole boundary $x = R$, equation (33) gives the stress concentrations factor $K_{\pi/2}$

$$K_{\pi/2} = \frac{\sigma_y(R,0)}{\sigma_\infty} = \frac{\sigma_\alpha}{\sigma_\infty} \Big|_{\alpha=\pi/2, \phi=0} = 1 + n \quad (34)$$

which agrees with equation (27) by setting $\alpha = \pi/2$ and $\phi = 0$. Equation (34) gives a constant value of $K_{\pi/2}$ for the same material regardless of the hole size. As the hole size decreases, the stress concentration factor $K_{\pi/2}$ decreases and finally approaches unity (that is, a plate without a hole). For composite materials, the hole-size effect on the stress concentration factor $K_{\pi/2}$ becomes significant when the hole diameter becomes less than 3.048 cm (1.2 in) (ref. 4).

To account for the hole-size effect in equation (34), two failure criteria were advanced by Whitney and Nuismer (ref. 5) for composite materials. Two theories are described in the following sections.

Point Stress Criterion

The point stress criterion assumes that the failure will occur when the stress $\sigma_y(x,0)$ at a certain small fixed distance (or characteristic distance) d_0 ahead of the hole boundary first reaches the tensile strength σ_f of the material (or tensile strength of the plate without a hole) (Fig. 3). Namely,

$$\sigma_y(x,0) \Big|_{x=R+d_0} = \sigma_f \quad (35)$$

Using this criterion and equation (33), the stress concentration factor, $K_{\pi/2}^{(1)}$, can be written as (ref. 5)

$$K_{\pi/2}^{(1)} = 1 + \frac{1}{2} \xi_1^2 + \frac{3}{2} \xi_1^4 - \frac{(1+n)-3}{2} (5 \xi_1^6 - 7 \xi_1^8) \quad (36)$$

where

$$\xi_1 \equiv \frac{R}{R+d_0} \quad (37)$$

For a large hole (that is $\xi_1 \rightarrow 1$), equation (36) gives

$$K_{\pi/2}^{(1)} \Big|_{\xi_1 \rightarrow 1} = K_{\pi/2} = 1+n \quad (38)$$

As the hole size decreases (that is, $\xi_1 \rightarrow 0$), equation (36) reduces to

$$K_{\pi/2}^{(1)} \Big|_{\xi_1 \rightarrow 0} = 1 \quad (39)$$

which corresponds to the case of no hole.

Average Stress Criterion

The average stress criterion assumes that failure will occur when the average value of $\sigma_y(x,0)$ over some small fixed distance a_0 ahead of the hole boundary first reaches the tensile strength of the material (without a hole) (fig. 3). Namely,

$$\frac{1}{a_0} \int_R^{R+a_0} \sigma_y(x,0) dx = \sigma_f \quad (40)$$

Using equations (33) and (40), the stress concentration factor $K_{\pi/2}^{(2)}$ can be written as (ref. 5)

$$K_{\pi/2}^{(2)} = \frac{1}{2(1 - \xi_2)} \left\{ 2 - \xi_2^2 - \xi_2^4 + [(1+n) - 3] \left(\xi_2^6 - \xi_2^8 \right) \right\} \quad (41)$$

$$= \frac{(1 + \xi_2)}{2} \left\{ 2 + \xi_2^2 + [(1+n) - 3] \xi_2^6 \right\} \quad (42)$$

where

$$\xi_2 \equiv \frac{R}{R + a_0} \quad (43)$$

For a large hole (that is, $\xi_2 \rightarrow 1$), equation (42) reduces to equation (34). Namely,

$$K_{\pi/2}^{(2)} \Big|_{\xi_2 \rightarrow 1} = K_{\pi/2} = 1 + n \quad (44)$$

And for the case without a hole (that is, $\xi_2 \rightarrow 0$), equation (42) gives

$$K_{\pi/2}^{(2)} \Big|_{\xi_2 \rightarrow 0} = 1 \quad (45)$$

The values of the characteristic distances d_0 and a_0 are determined by means of curve fitting of the experimental data obtained from tensile tests of rectangular specimens containing holes of different sizes. From literature surveys (refs. 4 and 5), the values of d_0 and a_0 for composite materials are in the ranges of

$$d_0 = 0.076 \text{ to } 0.127 \text{ cm (0.03 to 0.05 in)}$$

$$a_0 = 0.381 \text{ cm (0.15 in)}$$

EXPERIMENTS

The effect of hole size on the stress concentration factors predicted from the two theories discussed previously were examined by performing simple coupon tests. The widths W of the two rectangular specimens were $W = 3.81 \text{ cm (1.5 in)}$ and $W = 1.905 \text{ cm (0.75 in)}$. Both of the specimens contain small circular holes of $2R = 0.3175 \text{ cm (1/8 in)}$. The specimens were tested in a tensile test machine up to failure under uniaxial tension in the axis-1 direction, and the remote stress σ_∞ at the time of failure was calculated for each specimen. One specimen without a hole was also loaded up to failure in a similar manner to obtain the tensile strength, σ_f , of the material. The stress concentration factor $K_{\pi/2}$ for each specimen with a hole was calculated from

$$K_{\pi/2} = \frac{\sigma_f}{\sigma_\infty} \quad (46)$$

RESULTS

By replacing $\{E_1, E_2, G_{12}, \nu_{12}\}$, respectively, with $\{\bar{E}_1, \bar{E}_2, \bar{G}_{12}, \bar{\nu}_{12}\}$ in equations (27) and (28), the tangential stresses σ_α around a circular hole in a laminated HiMAT composite plate were calculated for three loading cases: $\phi = 0$ (loading in axis-1 direction), $\phi = \pi/4$, and $\phi = \pi/2$ (loading in axis-2 direction). Figure 4 shows the plots of σ_α for both the laminated HiMAT composite (eq. (27)) and isotropic materials (eq. (32)) when the plate is under uniaxial tension in the composite elastic axis-1 direction. The maximum stress concentration factor K for the laminated HiMAT composite reached the value 2.43 (less than 3) at four locations ($\alpha = \pm 65^\circ$ and $\alpha = \pm 115^\circ$) instead of two locations ($\alpha = \pm \pi/2$) for the isotropic case. When the loading axis is $\phi = \pi/4$ oblique to the composite axis 1 (fig. 5), the stress concentration factor K reaches the value of 3.49 (greater than 3) at two locations ($\alpha = 135^\circ$ and $\alpha = -45^\circ$). When the loading axis is parallel to the composite elastic axis 2 (fig. 6), the stress concentration factor K reaches the peak value of 2.44 (less than 3) at four locations ($\alpha = \pm 25^\circ$ and $\alpha = \pm 155^\circ$).

For comparison purposes, similar calculations were made for a single ply of the HiMAT composite using equation (27). When loading is along the fiber direction (axis 1, fig. 7), the stress concentration factor K reaches 10.20 at four locations ($\alpha = \pm 80^\circ$ and $\alpha = \pm 100^\circ$). When the loading is 45° oblique to the fiber direction (fig. 8), K reaches as high as 27.78 at two points ($\alpha = 114^\circ$ and $\alpha = -66^\circ$). When the loading direction is transverse to the fiber direction (fig. 9), the value of K reaches 6.81 at four points ($\alpha = \pm 55^\circ$ and $\alpha = \pm 125^\circ$). Tables 1 and 2 summarize the above results for both laminated and single-ply HiMAT composites. Notice that the laminated composite has much lower stress concentration factors than the single ply, indicating the improvement of the structural performance through the lamination process.

Figure 10 shows the plots of equations (36) and (42) for the laminated HiMAT composite $\left[n = \sqrt{2 \left(\frac{\bar{E}_1}{\bar{E}_2} - \bar{\nu}_{12} \right) + \frac{\bar{E}_1}{\bar{G}_{12}}} \right]$ taking the characteristic distances $d_o = 0.1016$ cm (0.04 in), $d_o = 0.127$ cm (0.05 in), and $a_o = 0.381$ cm (0.15 in) (refs. 4 and 5). For a hole diameter of 0.3175 cm (1/8 in), the predicted values of $K_{\pi/2}$ are summarized below.

d_o cm (in)	a_o cm (in)	$K_{\pi/2}$
0.0106 (0.04)	---	1.4367
0.1270 (0.05)	---	1.3152
---	0.3810 (0.15)	1.3498

The stress concentration factors $K_{\pi/2}$ determined from the uniaxial tensile tests (loading in axis-1 direction) of the laminated HiMAT composite specimens are tabulated below.

Specimen	W, cm (in)	2R, cm (in)	$K_{\pi/2}$
1	3.810 (0.75)	0.3175 (1/8)	1.333
2	1.905 (1.5)	0.3175 (1/8)	1.220

The above two data points are plotted in figure 10 and compare fairly well with the predicted curves, especially with the curves $d_0 = 0.127$ cm (0.05 in) and $a_0 = 0.381$ cm (0.15 in).

CONCLUDING REMARKS

Anisotropic plate theory was used to calculate the anisotropic stress concentration factors for single-ply and laminated HiMAT (highly maneuverable aircraft technology) research aircraft composite plates, each of which contained a circular hole. The analysis showed that the anisotropic stress concentration factor could be greater or less than three for anisotropic materials, (three is the stress concentration factor for isotropic materials) and the locations of the maximum tangential stress points could shift with the change of fiber orientation in relation to the loading axis. It was found that through the lamination process the stress concentration factor could be reduced drastically, and thereby the structural performance could be improved. The effect of the hole size on the stress concentration factor was examined in the light of the Point Stress Criterion and the Averaged Stress Criterion. The stress concentration factors calculated from these theories agree fairly well with the measured values for the hole size 0.3175 cm (1/8 in).

Ames Research Center
 Dryden Flight Research Facility
 National Aeronautics and Space Administration
 Edwards, California, February 21, 1984

REFERENCES

1. Calcote, L.R.: *The Analysis of Laminated Composite Structures*. Van Nostrand Reinhold Co., New York, 1969.
2. Jones, R.M.: *The Mechanics of Composite Materials*. McGraw-Hill Book Co., New York, 1975.
3. Lekhnitskii, S.G.; Tsai, S.W.; and Cheron, T.: *Anisotropic Plates*. Gordon and Breach Science Publishers, New York, 1968.
4. Nuismer, R.J.; and Whitney, J.M.: *Uniaxial Failure of Composite Laminates Containing Stress Concentrations*. *Fracture Mechanics of Composites*, ASTM ATP 593, pp. 117-142, 1975.
5. Whitney, J.M.; and Nuismer, R.J.: *Stress Fracture Criteria for Laminated Composite Containing Stress Concentration*. *J. Comp. Materials*, vol. 8, pp. 253-265, 1974.

TABLE 1. - STRESS CONCENTRATION FACTORS FOR A LAMINATED HIMAT COMPOSITE PLATE,
34 PLYS ($[\pm 50^\circ]_{14}, [-50^\circ]_{14}, [+35^\circ]_6$)

Orientation of loading axis, ϕ	0°	45°	90°
Stress concentration factor, K	2.43	3.49	2.44
Locations of peak tensile stress, α ..	$\pm 65^\circ, \pm 115^\circ$	$+135^\circ, -45^\circ$	$\pm 25^\circ, \pm 155^\circ$

TABLE 2. - STRESS CONCENTRATION FACTORS FOR A SINGLE PLY OF HIMAT COMPOSITE

Orientation of loading axis, ϕ	0°	45°	90°
Stress concentration factor, K	10.20	27.78	6.81
Locations of peak tensile stress, α ..	$\pm 80^\circ, \pm 100^\circ$	$+114^\circ, -66^\circ$	$\pm 55^\circ, \pm 125^\circ$

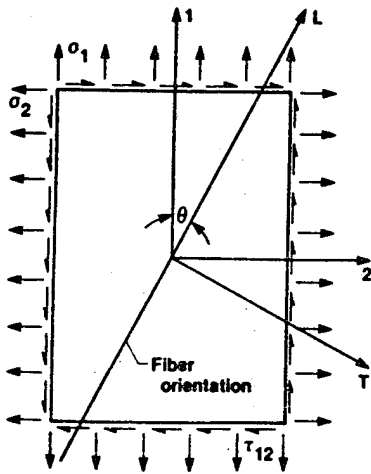


Figure 1. Single composite ply under combined loading.

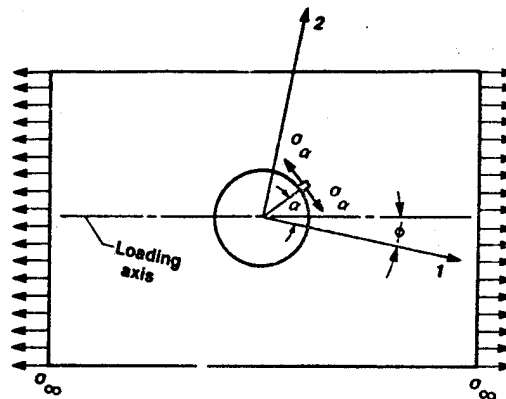


Figure 2. Tension at an angle to a principal elastic axis 1 of an anisotropic plate with a circular hole.

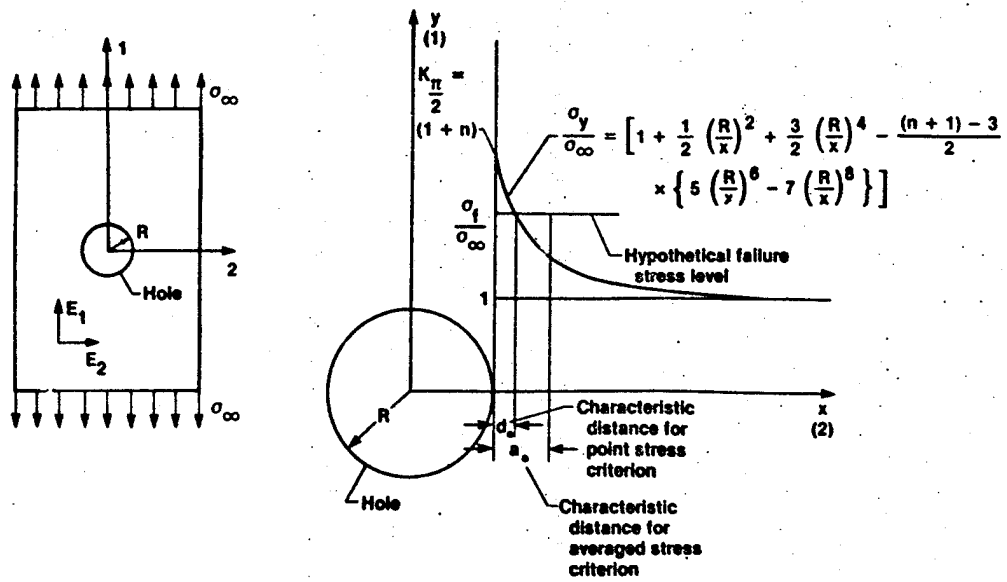


Figure 3. Failure hypothesis

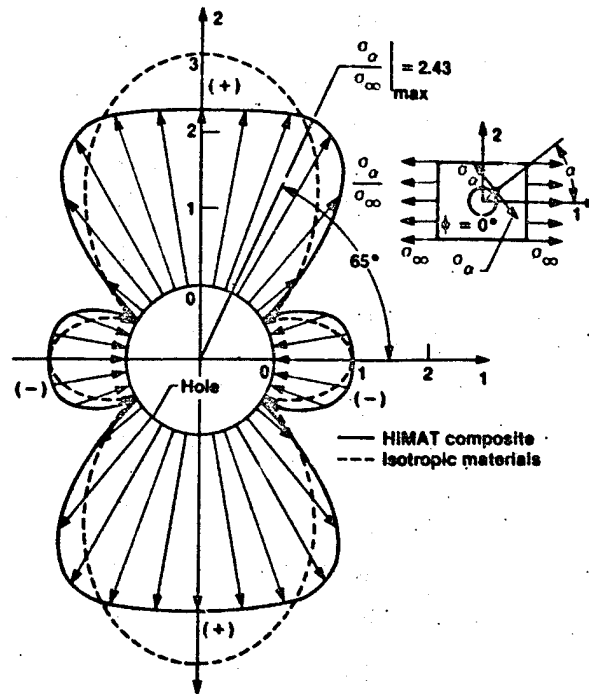


Figure 4. Tangential stress distribution around a circular hole in HIMAT composite plate [14 x (+50°)_S, 14 x (-50°)_S, 6 x (+35°)_S]. $\phi = 0^\circ$.

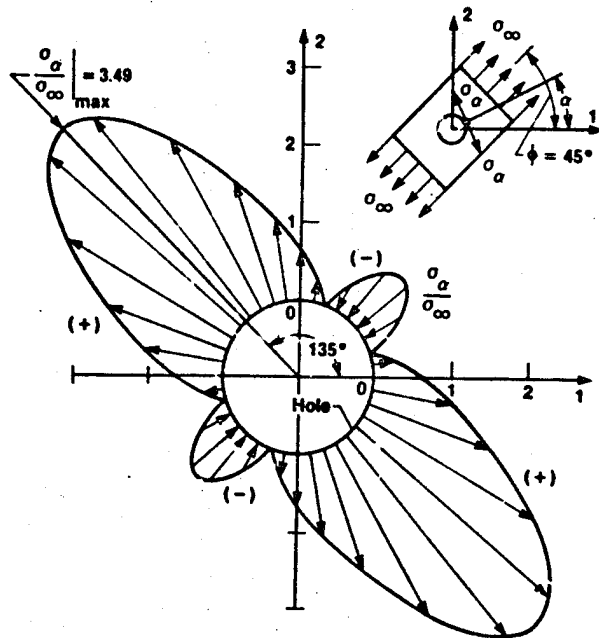


Figure 5. Tangential stress distribution around a circular hole in HINAT composite plate $[14 \times (+50^\circ)_S, 14 \times (-50^\circ)_S, 6 \times (+35^\circ)_S]$. $\phi = 45^\circ$.

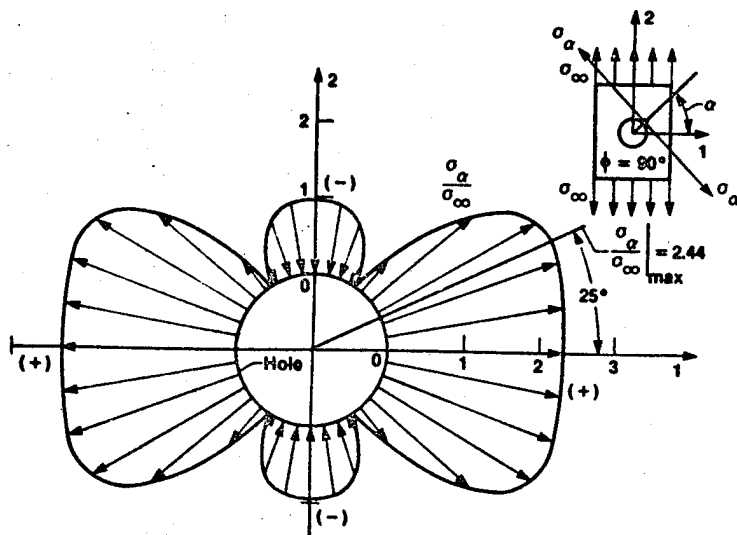


Figure 6. Tangential stress distribution around a circular hole in HINAT composite plate $[14 \times (+50^\circ)_S, 14 \times (-50^\circ)_S, 6 \times (+35^\circ)_S]$. $\phi = 90^\circ$.

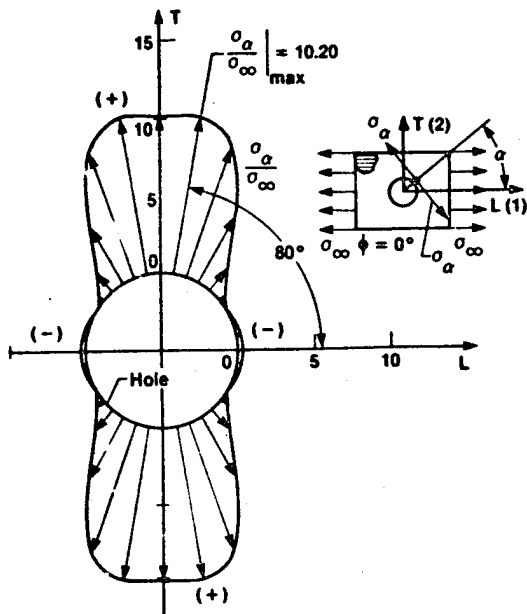


Figure 7. Tangential stress distribution around a circular hole in a single-ply composite plate. $\phi = 0^\circ$.

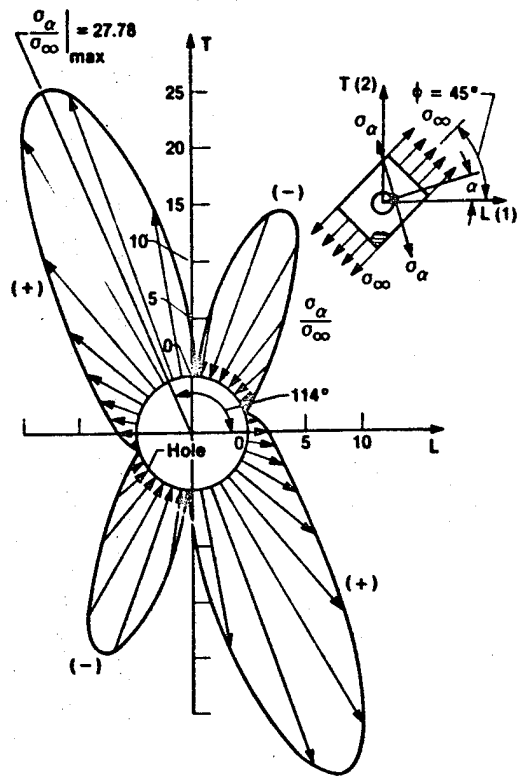


Figure 8. Tangential stress distribution around a circular hole in a single-ply composite plate. $\phi = 45^\circ$.

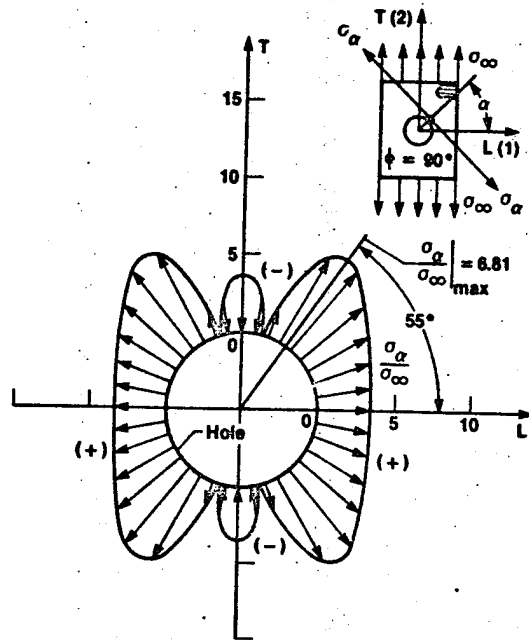


Figure 9. Tangential stress distribution around a circular hole in a single-ply composite plate. $\phi = 90^\circ$.

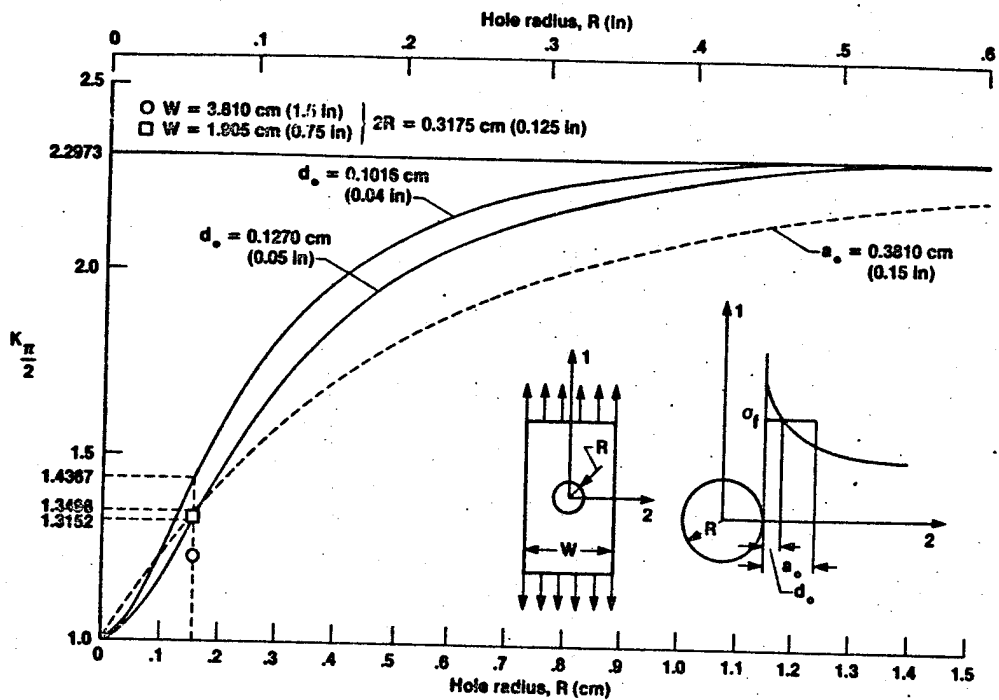


Figure 10. Stress concentration factor $K_T/2$ as a function of hole size.

1. Report No. NASA TM-86038	2. Government Accession No.	3. Recipient's Catalog No.	
4. Title and Subtitle STRESS CONCENTRATION AROUND A SMALL CIRCULAR HOLE IN THE HIMAT COMPOSITE PLATE		5. Report Date December 1985	6. Performing Organization Code
		8. Performing Organization Report No. H-1235	
7. Author(s) William L. Ko		10. Work Unit No. RTOP 533-02-71	11. Contract or Grant No.
9. Performing Organization Name and Address NASA Ames Research Center Dryden Flight Research Facility P.O. Box 273 Edwards, CA 93523		13. Type of Report and Period Covered Technical Memorandum	
		14. Sponsoring Agency Code	
12. Sponsoring Agency Name and Address National Aeronautics and Space Administration Washington, D.C. 20546		15. Supplementary Notes	
16. Abstract Anisotropic plate theory was used to calculate the anisotropic stress concentration factors for a composite plate (AS/3501-5 graphite/epoxy composite, single ply or laminated) containing a circular hole. This composite material was used on the highly maneuverable aircraft technology (HIMAT) vehicle. It was found that the anisotropic stress concentration factor could be greater or less than 3 (the stress concentration factor for isotropic materials), and that the locations of the maximum tangential stress points could shift with the change of fiber orientation with respect to the loading axis. The effect of hole size on the stress concentration factor was examined using the Point Stress Criterion and the Averaged Stress Criterion. The predicted stress concentration factors based on the two theories compared fairly well with the measured values for the hole size 0.3175 cm (1/8 in). It was also found that through the lamination process, the stress concentration factor could be reduced drastically, indicating an improvement in structural performance.			
17. Key Words (Suggested by Author(s)) Composite plates Stress concentrations Circular hole Hole size effect		18. Distribution Statement Unclassified-Unlimited STAR category 24	
19. Security Classif. (of this report) Unclassified	20. Security Classif. (of this page) Unclassified	21. No. of Pages 16	22. Price A02

*For sale by the National Technical Information Service, Springfield, Virginia 22161.